

## Supplementary Appendix

This appendix has been provided by the authors to give readers additional information about their work.

Supplement to: Zhao R, Follows GA, Beer PA, et al. Inhibition of the Bcl-x<sub>L</sub> deamidation pathway in myeloproliferative disorders. *N Engl J Med* 2008;359:2778-89.

## Supplementary data

Figure S1. FACS analysis of the cells purified from normal donors and CML patients.

(a) Granulocytes were purified from the peripheral blood of normal and CML patient donors. The similar cell surface marker phenotype of the normal and CML granulocytes was confirmed by staining with anti-CD2, CD3, CD19, conjugated to FITC; anti-CD13, conjugated to PE; and anti-CD14, conjugated to APC. The analysis was carried out on a FACScalibur.

(b) Peripheral blood mononuclear cells were isolated from CML patients and stained and analysed as in (a).

Figure S2. Expression levels of NHE-1 and extent of Bcl-x<sub>L</sub> deamidation in CML and PV patients.

(a) Western blots showing the NHE-1 expression level of representative CML patients and PV patients. Tubulin was reprobbed as a loading control. NHE-1 relative intensities normalised for protein loading are shown below the immunoblot with untreated controls set at a value of 1 (\*). Basal NHE-1 expression was comparable between normal donor, CML and PV cells.

(b) NHE-1 relative intensities (quantified from the western blots) of the normal donors, CML, and PV patients utilised in this study are shown as mean values with untreated controls set at a value of 1. Comparison of normal donors' and CML or PV patients' etoposide and irradiation treated sample values generates \* p<0.001.

(c) Percentages of deamidated Bcl-x<sub>L</sub> measured in aliquots of the samples used in (b) are shown as mean values. Comparison of normal donors' and CML or PV patients' etoposide and irradiation treated Bcl-x<sub>L</sub> deamidation values generates \* p<0.001.

There was no significant different in basal Bcl-x<sub>L</sub> deamidation values between donor, CML and PV patients' values (p = >0.05).

Figure S3. DNA damage induces the Bcl-x<sub>L</sub> deamidation pathway in T lymphocytes from CML and PV patients.

(a) DNA damage induces intracellular alkalinisation in T lymphocytes from CML and PV patients. PBMC were purified from patients' blood and stained with CD3-FITC,

before T cells were purified by flow cytometry. The cells were then processed as in Fig 1a . Intracellular pH was measured as in Fig 1b. The mean values  $\pm$  S.D. from 7 PV and 3 CML patients are shown in the histogram. \*  $p < 0.001$ .

(b) DNA damage induces Bcl-x<sub>L</sub> deamidation in T lymphocytes from CML and PV patients. Cell aliquots as used for (a) were subjected to immunoblotting for Bcl-x<sub>L</sub>. A representative blot is shown with actin as a loading control.

(c) DNA damage induces apoptosis in T lymphocytes from CML and PV patients. Apoptosis was measured using aliquots of the same cells used in (a) by sub-G1 DNA staining using flow cytometry. The mean values  $\pm$  S.D. from 7 PV and 3 CML patients are shown in the histogram. \* $p < 0.001$ .

Figure S4. Enforced intracellular alkalinisation of CML cells causes Bcl-x<sub>L</sub> deamidation and apoptosis.

(a) Enforced intracellular alkalinisation of CML cells causes Bcl-x<sub>L</sub> deamidation. Purified granulocytes from CML patients were cultured in RPMI/10% Fetal Calf Serum with the extracellular pH (pH<sub>e</sub>) as shown, treated with irradiation or etoposide as in Fig1a, and analysed for Bcl-x<sub>L</sub> deamidation by immunoblotting. The deamidated species of Bcl-x<sub>L</sub> were quantified as in Fig1a .

(b) Enforced intracellular alkalinisation of CML cells causes apoptosis. Aliquots of the cells used for (a) were assessed for apoptosis. The histograms represent sub-G1 % mean values  $\pm$  S.D. (n=10). The numbers above the histogram bars show the mean intracellular pH values. Statistical comparison of values between cells cultured in media with pH<sub>e</sub> 7.2 and pH<sub>e</sub> 8.0, and between cells cultured in media with pH<sub>e</sub> 7.2 and pH<sub>e</sub> 8.5, generated \*  $p < 0.001$ ; \*\*  $p < 0.0001$ .

Figure S5. Analysis of mutations in JAK2 from polycythaemia vera patients.

(a) Representative granulocyte sequencing traces from a normal control and 3 PV patient used in Figure 2, showing the somatic G to T transversion (black arrow) that causes phenylalanine to be substituted for valine at position 617 of JAK2 (V617F). (b) Pyrosequencing results for the PV patients are shown in the table. The allele burden was at least 62% in all patients. Since the granulocytes will include both homozygous and heterozygous mutant cells, these results indicate that the vast majority of granulocytes are likely to contain at least one mutant allele.

Figure S6. Enforced intracellular alkalinisation of polycythaemia vera cells causes Bcl-x<sub>L</sub> deamidation and apoptosis.

(a) Enforced intracellular alkalinisation of PV cells causes Bcl-x<sub>L</sub> deamidation. Purified granulocytes from PV patients were cultured in RPMI/10% Fetal Calf Serum with the extracellular pH (pH<sub>e</sub>) as shown, treated with irradiation or etoposide as in Fig1a, and analysed for Bcl-x<sub>L</sub> deamidation by immunoblotting. The deamidated species of Bcl-x<sub>L</sub> were quantified as in Fig1a .

(b) Enforced intracellular alkalinisation of PV cells causes apoptosis. Apoptosis (sub-G1) was measured using aliquots of the same cells used in (a), analysed as in Fig 1c. The histograms represent sub-G1 % mean values ± S.D. (n=8). The numbers above the histogram bars show the mean intracellular pH values. Statistical comparison of values between cells cultured in media with pH<sub>e</sub> 7.2 and pH<sub>e</sub> 8.0, and between cells cultured with pH<sub>e</sub> 7.2 and pH<sub>e</sub> 8.5, generated \* p<0.01; \*\* p<0.001.

Figure S7. Analysis of the Bcl-x<sub>L</sub> deamidation pathway in IMF patients' granulocytes.

(a) Granulocytes from 2 IMF patients without JAK2<sup>V617F</sup> mutation and 2 IMF patients with the JAK2<sup>V617F</sup> mutation were treated with etoposide and irradiation and analysed as in Fig 1a.

(b) Intracellular pH was measured using aliquots of the same cells used in (a).

(c) Apoptosis was measured using aliquots of the same cells used in (a) by sub-G1 DNA staining using flow cytometry.

Figure S8. Analysis of the Bcl-x<sub>L</sub> deamidation pathway in cancer cell lines.

(a) Representative western blots showing Bcl-x<sub>L</sub> deamidation in the 8 cell lines analysed. Cell lines were maintained in RPMI/10% Fetal Calf Serum. Cells were either treated with 50µM etoposide for 24h, or exposed to 5 Gy of irradiation and then cultured for 24h. Cells were lysed and subjected to immunoblotting for Bcl-x<sub>L</sub> and tubulin (loading control). The deamidated Bcl-x<sub>L</sub> values were calculated as in Fig 1a.

(b) Intracellular pH was measured in the same cell aliquots from (a) as for Fig. 1b.

(c) Apoptosis (sub-G1 percentages) was measured in the same cell aliquots from (a) as for Fig. 1c. The histograms in both (b) and (c) show the mean values  $\pm$  S.D. from at least 3 separate measurements.

Figure S9. Kinase expression levels correlate with the degree of inhibition of DNA damage-induced Bcl-x<sub>L</sub> deamidation.

(a) Flow cytometric analysis of sub-populations of BaF3/TpoR cells transfected with different expression levels of Bcr-Abl. Retroviral vector MIG-BCR-ABL was transduced into Baf3/TPoR cells at a range of retroviral titers. The cells were then sorted using a FACSAria into four populations with different expression levels of GFP.

(b) The four populations of cells from (a) were processed for immunoblotting with a BCR-ABL antibody and the immunoblots reprobed for actin as loading control.

(c) The BCR-ABL expression level correlates with the degree of inhibition of DNA damage-induced Bcl-x<sub>L</sub> deamidation. The same cell aliquots as shown in (b) were treated with etoposide and irradiation as in Fig 1a, and processed for immunoblotting with Bcl-x<sub>L</sub>. One representative blot from 3 independent experiments is shown and the percentage of deamidation was quantified as in Fig 1a.

(d) The BCR-ABL expression level correlates with the degree of inhibition of DNA damage-induced intracellular alkalinisation. Intracellular pH was measured in the same cell aliquots as in (b). The mean values  $\pm$  S.D. from 3 independent experiments are shown in the histogram.

(e) Jak2<sup>V617F</sup> and NPM-ALK were expressed in Baf3/TpoR cells by retroviral transduction. Three cell populations with different GFP levels (labelled as #1, #2 and #3) were sorted by flow cytometry from each kinase-transduced Baf3/TpoR cells.

(f) A comparison of different BCR-ABL, mutant Jak2 and NPM-ALK expression levels on the DNA damage-induced Bcl-x<sub>L</sub> deamidation pathway. Cells expressing Jak2<sup>V617F</sup> and NPM-ALK shown in (e) and cells expressing BCR-ABL shown in (a) and (b) were treated with etoposide for 24h, then processed for immunoblotting with Bcl-x<sub>L</sub>. A representative blot is shown with the percentage of deamidation below. Note that with increased kinase expression, Jak2<sup>V617F</sup> and BCR-ABL show increased inhibition of the pathway, whereas NPM-ALK shows no inhibition even at its highest expression level..

Figure S10. DNA damage-triggered apoptosis in normal CD34-positive cells is inhibited by DMA.

CD34-positive cells from three normal donors were treated with or without DMA (100  $\mu$ M), and with or without etoposide (50 $\mu$ M) for 24 h. Percentage of sub-G1 DNA was measured by FACS. Statistical evaluation of the difference between 'etoposide alone' and 'etoposide+DMA' generated  $p = <0.05$ .

Figure S11. JAK2 inhibitors (JAK inhibitor 1, TG101209 and AT9283) reverse the inhibition of the DNA damage-induced Bcl-x<sub>L</sub> deamidation pathway in PV granulocytes.

(a) JAK2 inhibitors reverse the inhibition of DNA damage-induced intracellular alkalinisation in PV granulocytes. Intracellular pH was measured using aliquots of the same cells used in Fig 3f. The mean values  $\pm$  S.D. from 3 PV patients are shown in the histogram. Statistical comparison of values in the presence or absence of JAK2 inhibitors revealed  $p = <0.01$ .

(b) JAK2 inhibitors reverse the inhibition of DNA damage-induced apoptosis in PV granulocytes. Apoptosis was measured using aliquots of the same cells used in Fig 3f by sub-G1 DNA staining using flow cytometry. The mean values  $\pm$  S.D. from 3 PV patients are shown in the histogram. Statistical comparison of values in the presence or absence of JAK2 inhibitors revealed  $p = <0.01$ .

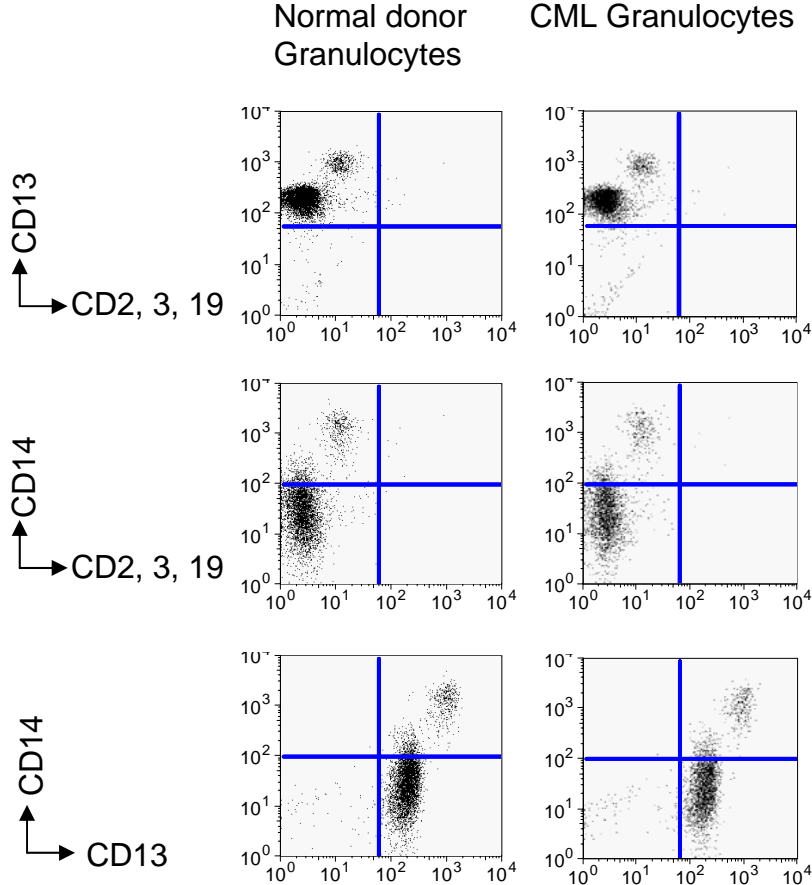
**Figure S12. Enforced intracellular alkalinisation reverses the effects of imatinib-resistance in CML cells.**

(a) Enforced intracellular alkalinisation of imatinib-resistant CML cells causes Bcl-x<sub>L</sub> deamidation. PBMCs from an imatinib-resistant CML patient were cultured in RPMI/10% Fetal Calf Serum with the extracellular pH (pH<sub>e</sub>) as shown, treated with irradiation or etoposide as in Fig 1a, and analysed for Bcl-x<sub>L</sub> deamidation by immunoblotting. The deamidated species of Bcl-x<sub>L</sub> were quantified as in Fig. 1a.

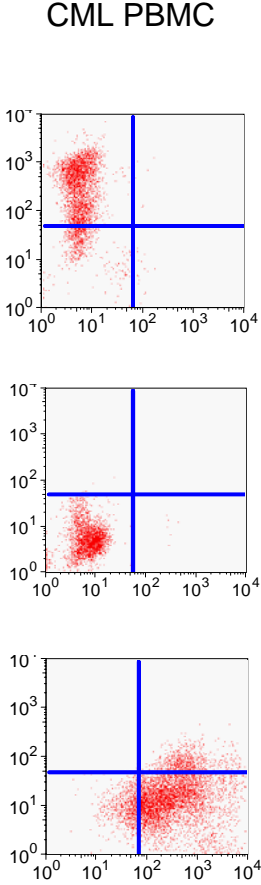
(b) The intracellular pH and apoptosis (sub-G1 percentage) were measured in the same cell aliquots as in Fig 1 (b) and (c) respectively. The numbers above the histogram bars show the mean intracellular pH values.

Supplementary Figure S1

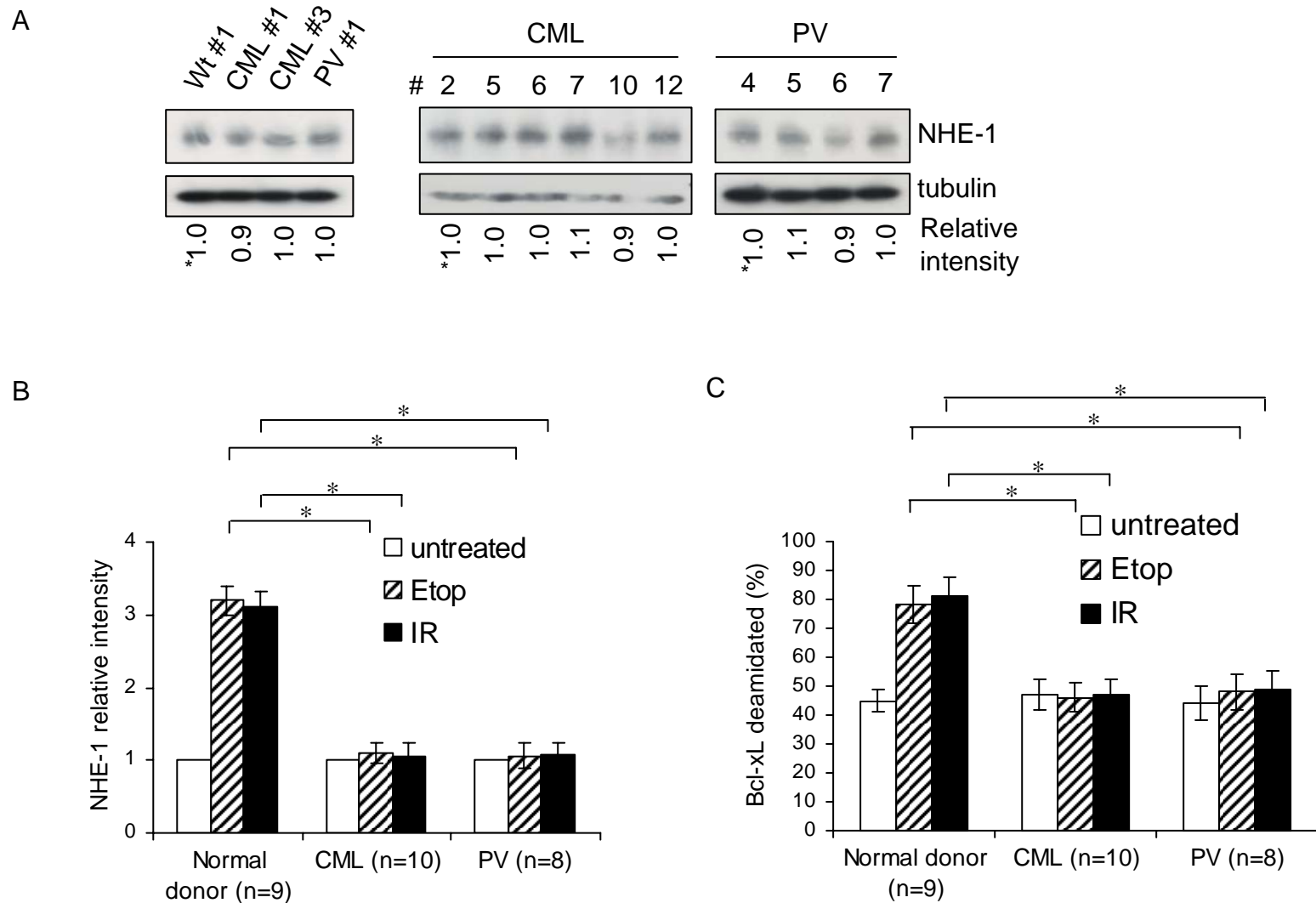
A



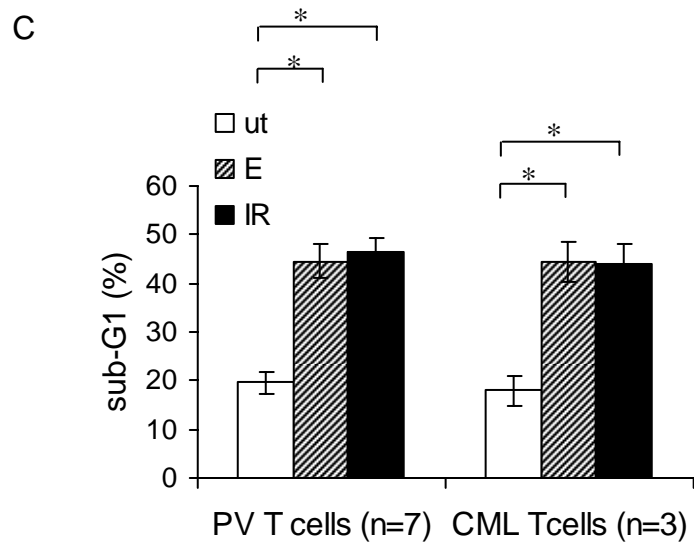
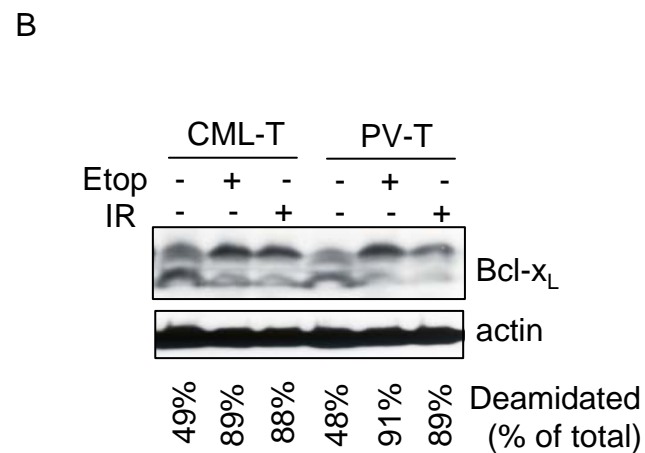
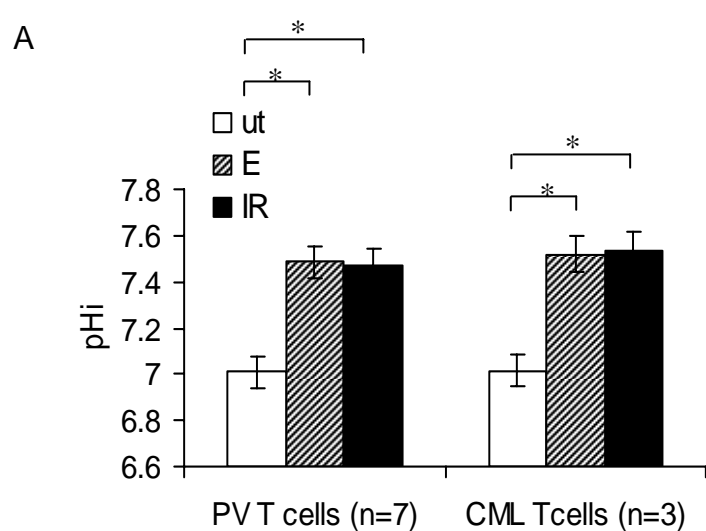
B



## Supplementary Figure S2

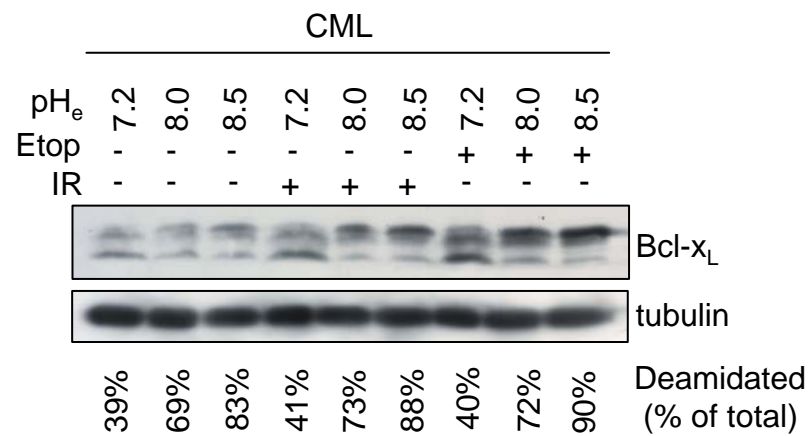


### Supplementary Figure S3

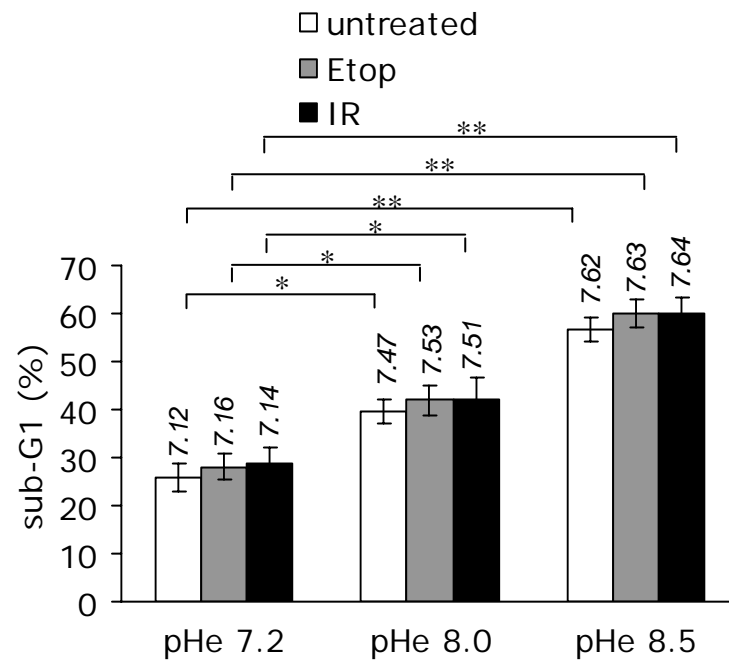


# Supplementary Figure S4

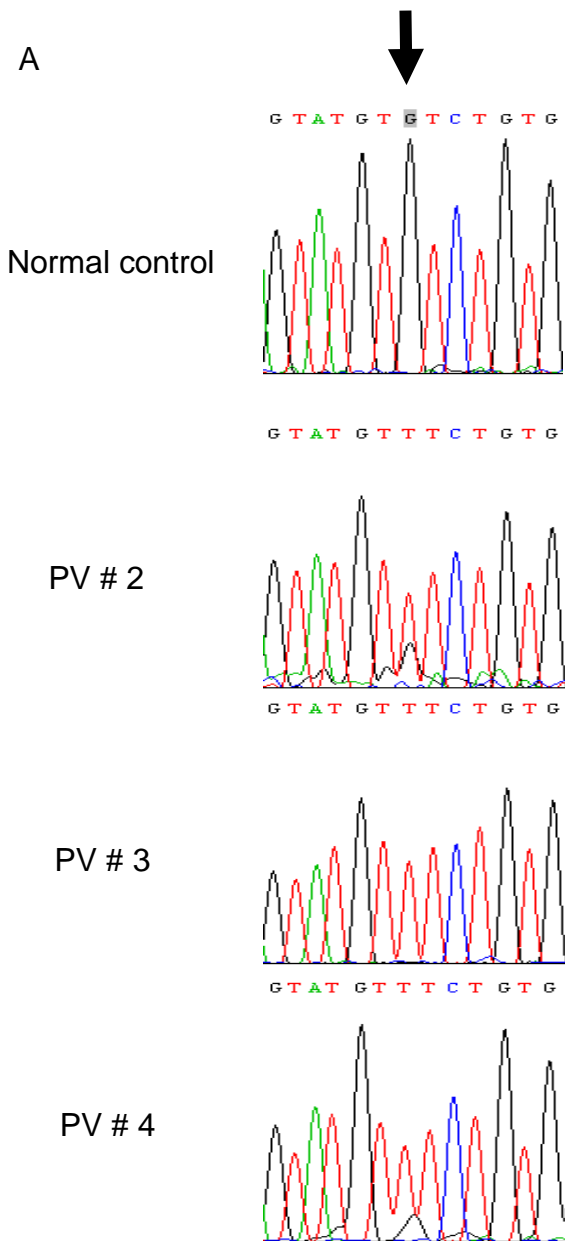
A



B



# Supplementary Figure S5

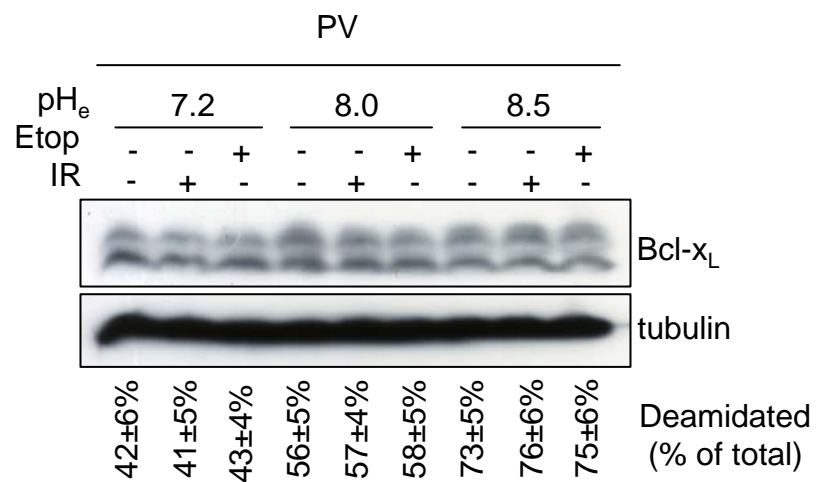


B

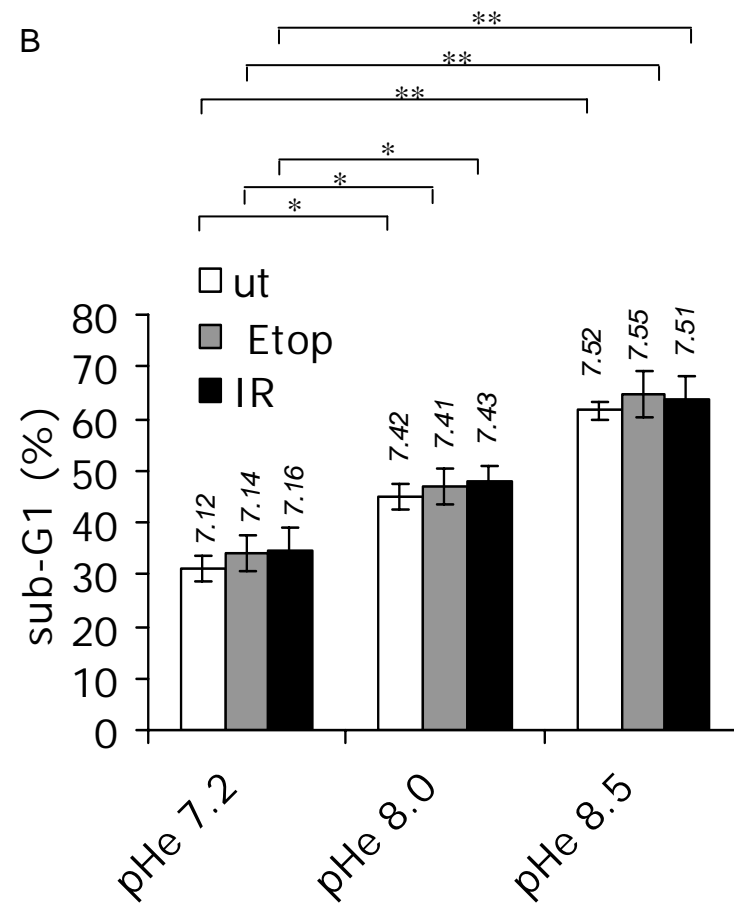
Patient No.	Mutant allele burden
#1	90%
#2	96%
#3	93%
#4	100%
#5	72%
#6	98%
#7	77%
#8	62%

# Supplementary Figure S6

A

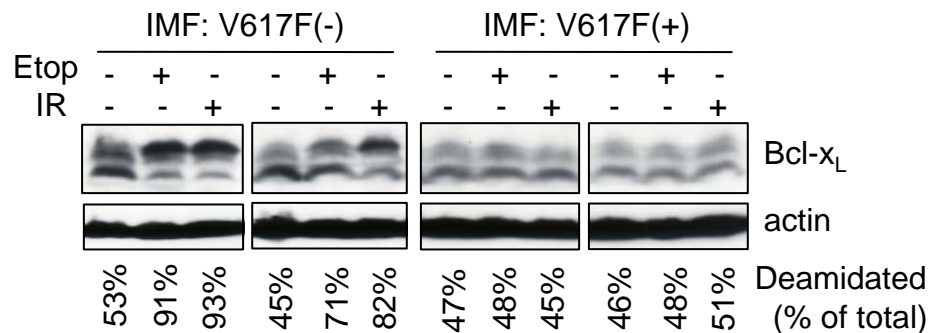


B

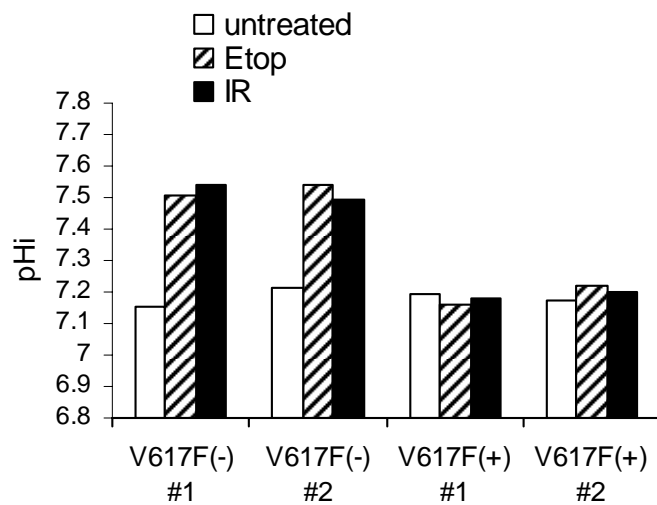


# Supplementary Figure S7

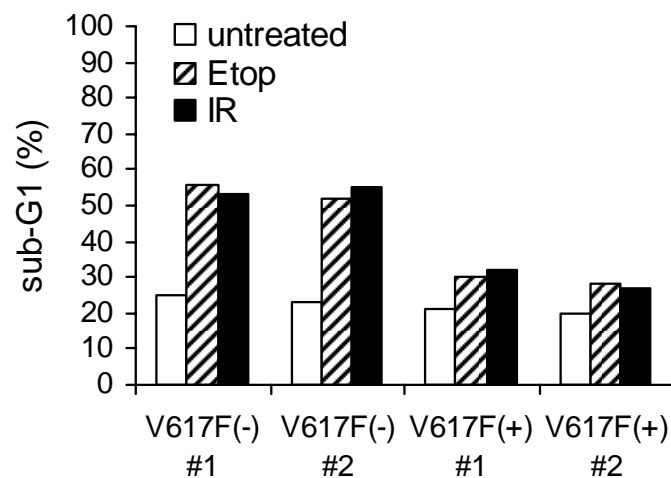
A



B

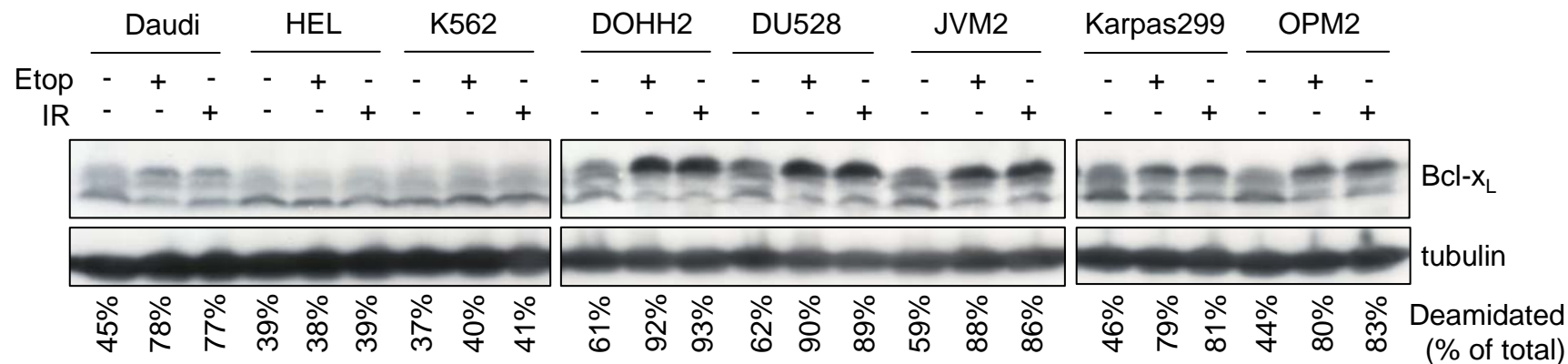


C

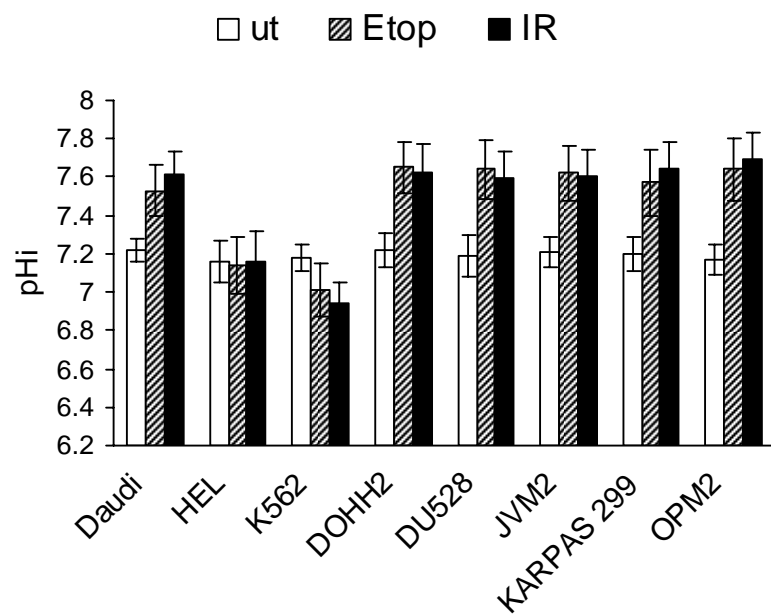


# Supplementary Figure S8

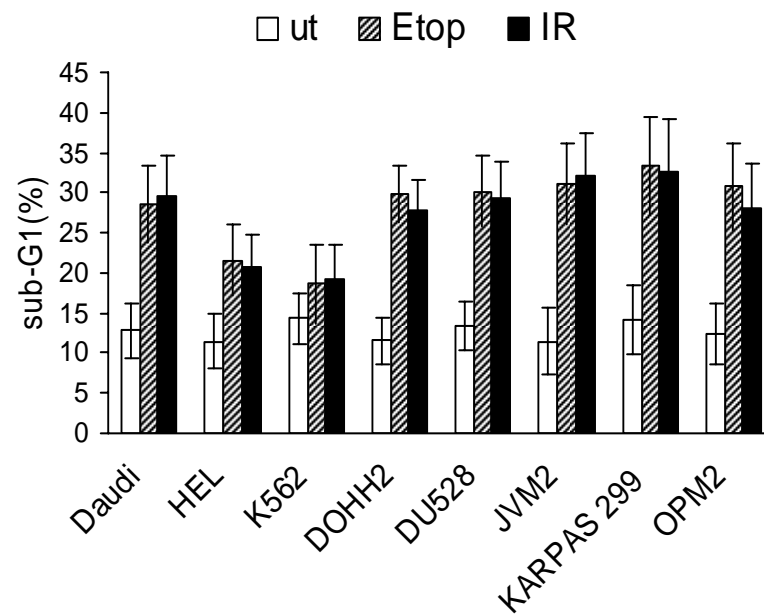
A



B

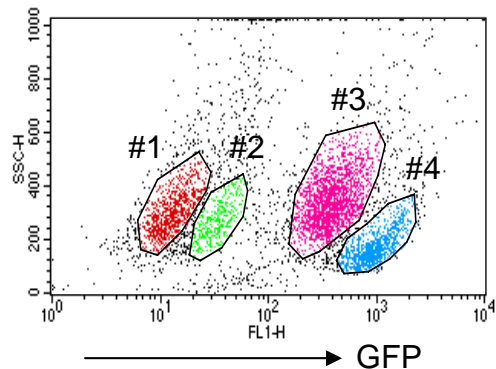


C

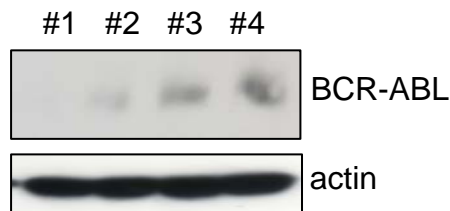


# Supplementary Figure S9

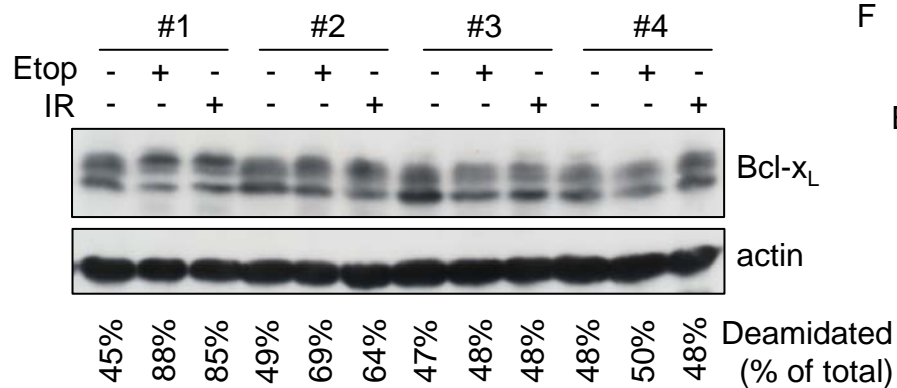
A



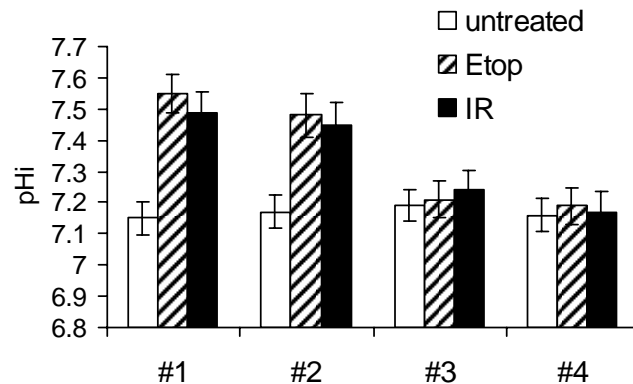
B



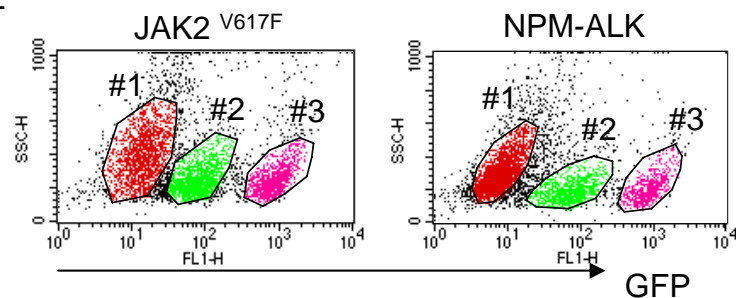
C



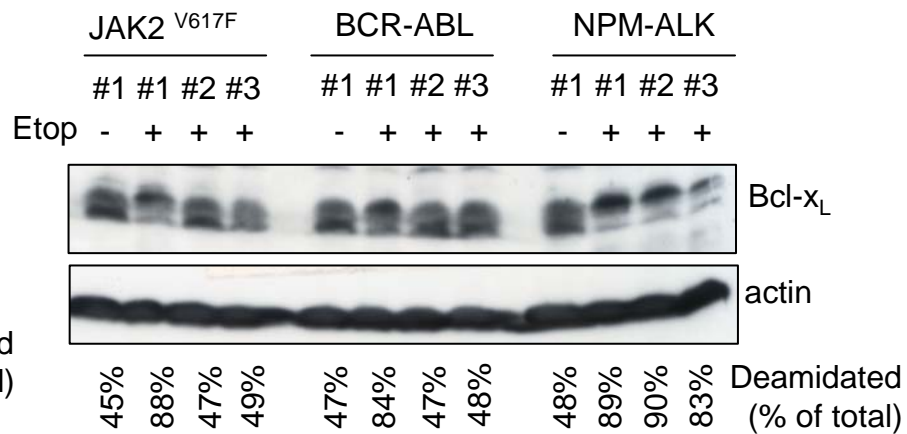
D



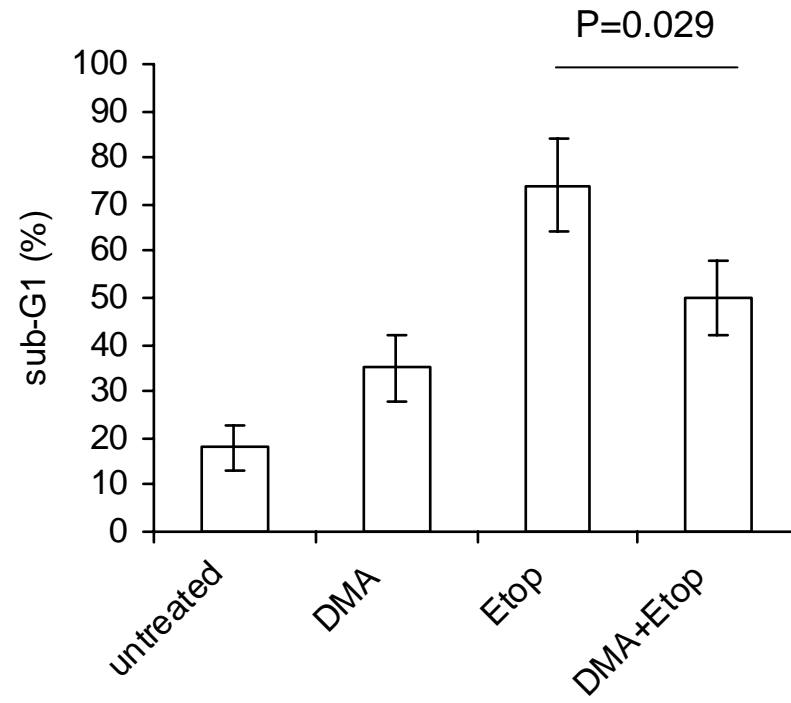
E



F

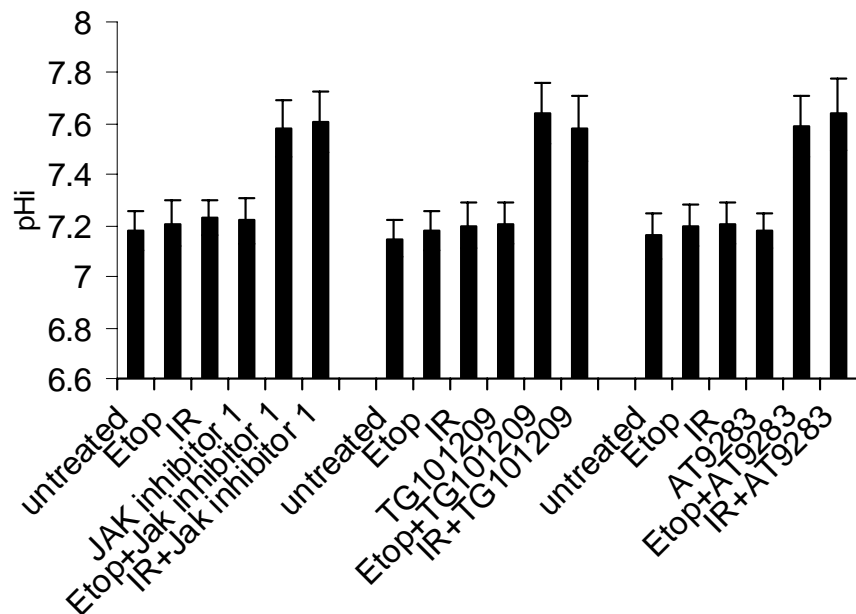


Supplementary Figure S10

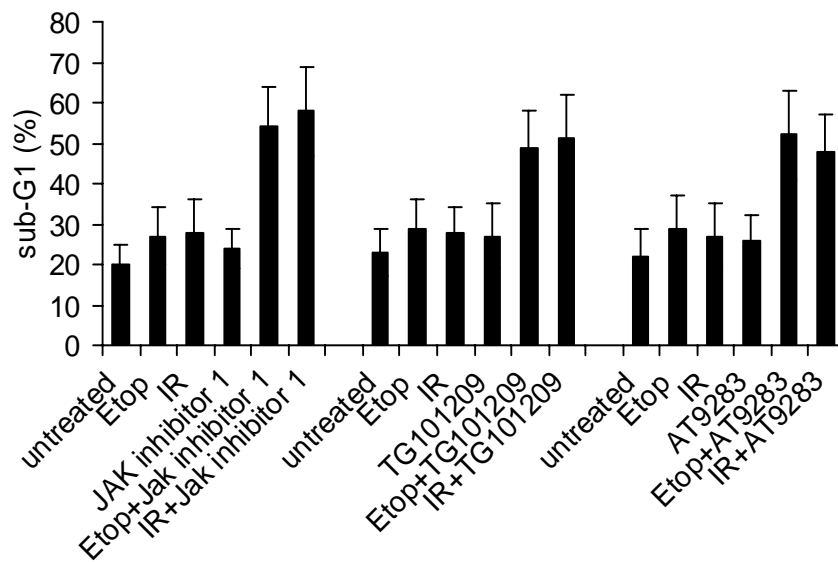


# Supplementary Figure S11

A

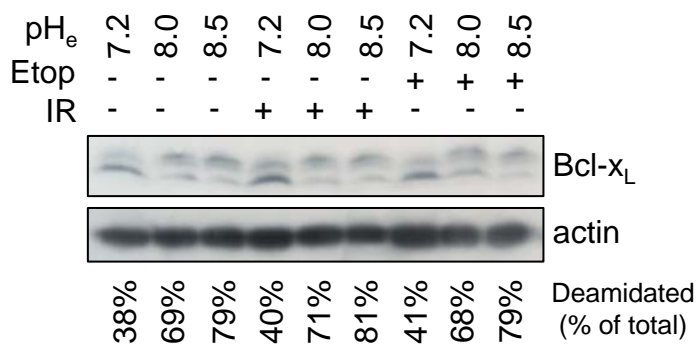


B

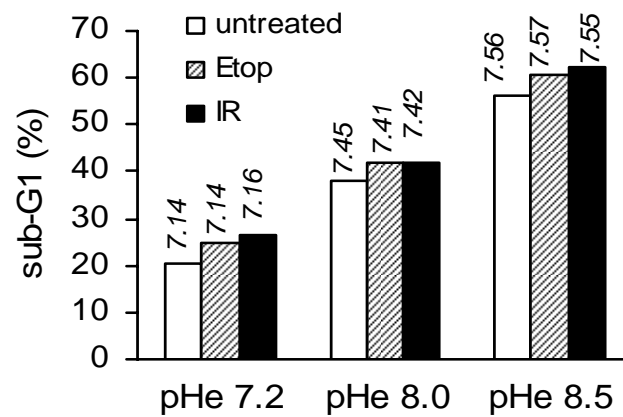


# Supplementary Figure S12

A



B



**Supplementary Table 1. Description of cell lines used for investigation of the Bcl-x<sub>L</sub> deamidation pathway**

Cell lines	Hematological cancers	Chromosomal defects	Dysfunctional / deregulated gene
K562 <sup>1</sup>	Chronic Myeloid Leukaemia	t(9;22)(q34;q11)	BCR-ABL*
HEL <sup>2</sup>	Polycythaemia Vera	JAK2 V617F homozygous	JAK2*
Daudi <sup>3</sup>	Burkitt lymphoma/Burkitt cell leukemia	t(8;14)(q24;q32)	c-myc
DU528 <sup>4</sup>	Precursor T-cell acute lymphoblastic leukemia	t(1;14)(p34;q11)	TAL1
JVM2 <sup>5</sup>	Mantle-cell lymphoma	t(11;14)(q13;q32)	cyclinD1
Karpas299 <sup>6</sup>	Anaplastic large-cell lymphoma	t(2;5)(p23;q35)	NPM-ALK*
OPM2 <sup>7</sup>	Multiple myeloma	t(4;14)(p16;q32)	FGFR3*
DOHH2 <sup>8</sup>	Follicular lymphoma	t(14;18)(q32;q21)	BCL2

\* signifies dysfunctional / deregulated gene is a tyrosine kinase

1. Lozzio, C.B. & Lozzio, B.B. Human chronic myelogenous leukemia cell-line with positive Philadelphia chromosome. *Blood* **45**, 321-34 (1975).
2. Martin, P. & Papayannopoulou, T. HEL cells: a new human erythroleukemia cell line with spontaneous and induced globin expression. *Science* **216**, 1233-5 (1982).
3. Klein, E. et al. Surface IgM-kappa specificity on a Burkitt lymphoma cell in vivo and in derived culture lines. *Cancer Res* **28**, 1300-10 (1968).
4. Begley, C.G. et al. The gene SCL is expressed during early hematopoiesis and encodes a differentiation-related DNA-binding motif. *Proc Natl Acad Sci U S A* **86**, 10128-32 (1989).
5. Melo, J.V. et al. Two new cell lines from B-prolymphocytic leukaemia: characterization by morphology, immunological markers, karyotype and Ig gene rearrangement. *Int J Cancer* **38**, 531-8 (1986).
6. Fischer, P. et al. A Ki-1 (CD30)-positive human cell line (Karpas 299) established from a high-grade non-Hodgkin's lymphoma, showing a 2;5 translocation and rearrangement of the T-cell receptor beta-chain gene. *Blood* **72**, 234-40 (1988).
7. Chesi, M. et al. Frequent translocation t(4;14)(p16.3;q32.3) in multiple myeloma is associated with increased expression and activating mutations of fibroblast growth factor receptor 3. *Nat Genet* **16**, 260-4 (1997).
8. Kluin-Nelemans, H.C. et al. A new non-Hodgkin's B-cell line (DoHH2) with a chromosomal translocation t(14;18)(q32;q21). *Leukemia* **5**, 221-4 (1991).